CHAPTER 3.

Broad-Scale Patterns of Forest Fire Occurrence across the 50 United States and the Caribbean Territories, 2019

Kevin M. Potter

INTRODUCTION

As a pervasive disturbance agent operating at many spatial and temporal scales, wildland fire is a key abiotic factor affecting forest health both positively and negatively. In some ecosystems, for example, wildland fires have been essential for regulating processes that maintain forest health (Lundquist and others 2011). Wildland fire is an important ecological mechanism that shapes the distributions of species, maintains the structure and function of fire-prone communities, and acts as a significant evolutionary force (Bond and Keeley 2005). At the same time, wildland fires have created forest health (i.e., sustainability) problems in some ecosystems (Edmonds and others 2011).

Current fire regimes on more than half of the forested area in the conterminous United States have been moderately or significantly altered from historical regimes (Barbour and others 1999), potentially altering key ecosystem components such as species composition, structural stage, stand age, canopy closure, and fuel loadings (Schmidt and others 2002). Fires in some regions and ecosystems have become larger, more intense, and more damaging because of the accumulation of fuels as a result of prolonged fire suppression (Pyne 2010). In some regions, plant communities have experienced or are undergoing rapid compositional and structural changes as a result of fire suppression (Nowacki and Abrams 2008). Additionally, changes in fire intensity and recurrence could result in decreased forest resilience and persistence (Lundquist and others 2011), and fire regimes altered by global climate change could cause large-scale shifts in vegetation spatial patterns (McKenzie and others 1996).

At the same time, large wildland fires also can have long-lasting social and economic consequences, which include the loss of human life and property, smoke-related human health impacts, and the economic cost and dangers of fighting the fires themselves (Gill and others 2013, Richardson and others 2012).

This chapter presents analyses of daily satellite-based fire occurrence data that map and quantify the locations and intensities of fire occurrences spatially across the conterminous United States, Alaska, Hawaii, and the Caribbean territories in 2019. It also compares 2019 fire occurrences, within a geographic context, to all the recent years for which such data are available. Quantifying and monitoring such large-scale patterns of fire occurrence across the United States can help improve our understanding of the ecological and economic impacts of fire as well as the appropriate management and prescribed use of fire. Specifically, large-scale assessments of fire occurrence can help identify areas where specific management activities may be needed, or where research into the ecological and socioeconomic impacts of fires may be required. Additionally, given the potential for climate change and shifting species distributions to alter historic fire regimes, quantifying the location and frequency

of forest fire occurrences across the United States can help us to better understand emerging spatiotemporal patterns of fire occurrence.

METHODS

Data

Annual monitoring and reporting of active wildland fire events using the Moderate Resolution Imaging Spectroradiometer (MODIS) Active Fire Detections for the United States database (USDA Forest Service 2020) allow analysts to spatially display and summarize fire occurrences across broad geographic regions (Coulston and others 2005; Potter 2012a, 2012b, 2013a, 2013b, 2014, 2015a, 2015b, 2016, 2017, 2018, 2019, 2020a). A fire occurrence is defined as one daily satellite detection of wildland fire in a 1-km pixel, with multiple fire occurrences possible on a pixel across multiple days resulting from a single wildland fire that lasts more than 1 day. The data are derived using the MODIS Rapid Response System (Justice and others 2002, 2011) to extract fire location and intensity information from the thermal infrared bands of imagery collected daily by two satellites at a resolution of 1 km, with the center of a pixel recorded as a fire occurrence (USDA Forest Service 2020). The Terra and Aqua satellites' MODIS sensors identify the presence of a fire at the time of image collection, with Terra observations collected in the morning and Aqua observations collected in the afternoon. The resulting fire occurrence data represent only whether a fire was active because the MODIS data bands may not differentiate between a hot fire in a relatively small area (0.01 km^2, for example) and a cooler fire over a larger area (1 km^2, for example) if the foreground to background temperature contrast is not sufficiently high. The MODIS Active Fire database does well at capturing large fires during cloud-free conditions but may underrepresent rapidly burning, small, and low-intensity fires, as well as fires in areas with frequent cloud cover (Hawbaker and others 2008). For large-scale assessments, the dataset represents a good alternative to the use of information on ignition points, which may be preferable but can be difficult to obtain or may not exist (Tonini and others 2009). More information about the performance of this product is available in Justice and others (2011). The fire occurrence data additionally do not identify fires intentionally set for management purposes (controlled burns), which are common in some parts of the United States, particularly in the South.

It is important to underscore that estimates of burned area and calculations of MODIS-detected fire occurrences are two different metrics for quantifying fire activity within a given year. Most importantly, the MODIS data contain both spatial and temporal components because persistent fire will be detected repeatedly over several days on a given 1-km pixel. In other words, a location can be counted as having a fire occurrence multiple times, once for each day a fire is detected at the location. Analyses of the MODIS-detected fire occurrences, therefore, measure the total number of daily

1-km pixels with fire during a year, as opposed to quantifying only the area on which fire occurred at some point during the course of the year. A fire detected on a single pixel for every day in the month of July, for example, would be equivalent to 31 fire occurrences.

The Terra and Aqua satellites, which carry the MODIS sensors, were launched in 1999 and 2002, respectively, and will eventually be decommissioned. An alternative fire occurrence data source is the Visible Infrared Imaging Radiometer Suite (VIIRS) sensor on board the Suomi National Polar-orbiting Partnership (Suomi NPP) weather satellite. The transition to this new data source will require a comparison of fire occurrence detections between it and MODIS. This is because VIIRS data are available from 2014 onward (USDA Forest Service 2020), but it will be important for assessments of fire occurrence trends to be able to analyze as long a window of time as possible (i.e., from the beginning of MODIS data availability).

Analyses

These MODIS products for 2019, and for the 18 preceding full years of data, were processed in ArcMap® (ESRI 2017) to determine forest fire occurrence density (that is, the number of fire occurrences/100 km^2 [10 000 ha] of tree canopy cover area) for each ecoregion section in the conterminous United States (Cleland and others 2007), for ecoregions on each of the major islands of Hawaii (Potter 2020b), and for the islands of the Caribbean territories of Puerto Rico and the U.S. Virgin Islands. For the current analyses, the forest fire occurrence density metrics for the conterminous 48 States, Hawaii, and the Caribbean territories (the number of fire occurrences/100 km^2 of tree canopy cover area) were calculated after screening out wildland fires that did not intersect with tree canopy data. The tree canopy data had been resampled to 240 m from a 30-m raster dataset that estimates percentage of tree canopy cover (from 0 to 100 percent) for each grid cell; this dataset was generated from the 2011 National Land Cover Database (NLCD) (Homer and others 2015) through a cooperative project between the Multi-Resolution Land Characteristics Consortium and the U.S. Department of Agriculture Forest Service, Geospatial Technology and Applications Center (GTAC) (Coulston and others 2012). For our purposes, we treated any cell with >0-percent tree canopy cover as forest. Comparable tree canopy cover data were not available for Alaska, so we instead created a 240-m-resolution layer of forest and shrub cover from the 2011 NLCD. The MODIS fire occurrence detection data were then intersected with this layer and with ecoregion sections for the State (Spencer and others 2002) to calculate the number of fire occurrences/100 km^2 of forest and shrub cover within each ecoregion section in Alaska. In Forest Health Monitoring national reports before 2019, the number of fire occurrences/100 km^2 of forest was determined for the conterminous States, Alaska, and Hawaii using a forest cover mask derived from MODIS imagery by the Forest Service GTAC (USDA Forest Service 2008).

The total numbers of forest fire occurrences were also determined separately for the conterminous States, Alaska, Hawaii, and the Caribbean territories after clipping the MODIS fire occurrences by the canopy cover or tree and shrub cover data.

The fire occurrence density value for each of the ecoregions of the States and for the Caribbean islands in 2019 was then compared with the mean fire density values for the first 18 full years of MODIS Active Fire data collection (2001–2018). Specifically, the difference of the 2019 value and the previous 18-year mean for an ecoregion was divided by the standard deviation across the previous 18-year period, assuming a normal distribution of fire density over time in the ecoregion. The result for each ecoregion was a standardized *z*-score, which is a dimensionless quantity describing the degree to which the fire occurrence density in the ecoregion in 2019 was higher, lower, or the same relative to all the previous years for which data have been collected, accounting for the variability in the previous years. The *z*-score is the number of standard deviations between the observation and the mean of the historic observations in the previous years. Approximately 68 percent of observations would be expected within one standard deviation of the mean, and 95 percent within two standard deviations. Near-normal conditions are classified as those within a single standard deviation of the mean, although such a threshold is somewhat arbitrary. Conditions between about one and two standard deviations of the mean are moderately different from mean conditions but are not significantly different statistically. Those outside about two standard deviations would be considered statistically greater than or less than the long-term mean (at $p < 0.025$ at each tail of the distribution).

Additionally, we used the Spatial Association of Scalable Hexagons (SASH) analytical approach to identify forested areas in the conterminous United States with higher-than-expected fire occurrence density in 2019. This method identifies locations where ecological phenomena occur at greater or lower occurrences than expected by random chance and is based on a sampling frame optimized for spatial neighborhood analysis, adjustable to the appropriate spatial resolution, and applicable to multiple data types (Potter and others 2016). Specifically, it consists of dividing an analysis area into scalable equal-area hexagonal cells within which data are aggregated, followed by identifying statistically significant geographic clusters of hexagonal cells within which mean values are greater or less than those expected by chance. To identify these clusters, we employed a Getis-Ord G_i^* hot spot analysis (Getis and Ord 1992) in ArcMap® 10.5.1 (ESRI 2017).

The spatial units of analysis were 9,810 hexagonal cells, each approximately 834 km^2 in area, generated in a lattice across the conterminous United States using intensification of the Environmental Monitoring and Assessment Program (EMAP) North American hexagon coordinates (White and others 1992). These coordinates are the foundation of a sampling frame in which a hexagonal lattice

was projected onto the conterminous United States by centering a large base hexagon over the region (Reams and others 2005, White and others 1992). The hexagons are compact and uniform in their distance to the centroids of neighboring hexagons, meaning that a hexagonal lattice has a higher degree of isotropy (uniformity in all directions) than does a square grid (Shima and others 2010). These are convenient and highly useful attributes for spatial neighborhood analyses. These scalable hexagons also are independent of geopolitical and ecological boundaries, avoiding the possibility of different sample units (such as counties, States, or watersheds) encompassing vastly different areas (Potter and others 2016). We selected hexagons 834 km^2 in area because this is a manageable size for making monitoring and management decisions in analyses across the conterminous United States (Potter and others 2016).

Fire occurrence density values for each hexagon were quantified as the number of forest fire occurrences/100 km^2 of tree canopy cover area within the hexagon. The Getis-Ord G_i^* statistic was used to identify clusters of hexagonal cells with fire occurrence density values higher than expected by chance. This statistic allows for the decomposition of a global measure of spatial association into its contributing factors, by location, and is therefore particularly suitable for detecting outlier assemblages of similar conditions in a dataset, such as when spatial clustering is concentrated in one subregion of the data (Anselin 1992).

Briefly, G_i^* sums the differences between the mean values in a local sample, determined in this case by a moving window of each hexagon and its 18 first- and second-order neighbors (the 6 adjacent hexagons and the 12 additional hexagons contiguous to those 6) and the global mean of the 9,644 hexagonal cells with tree canopy cover (of the total 9,810) in the conterminous United States. As described in Laffan (2006), it is calculated as

$$G_i^*(\boldsymbol{d}) = \frac{\sum_j w_{ij}(\boldsymbol{d})\, x_j - W_i^* \bar{x}^*}{s^* \sqrt{\frac{(ns_{1i}^*) - W_i^{*2}}{n-1}}}$$

where

G_i^* = the local clustering statistic (in this case, for the target hexagon)

i = the center of local neighborhood (the target hexagon)

d = the width of local sample window (the target hexagon and its first- and second-order neighbors)

x_j = the value of neighbor j

w_{ij} = the weight of neighbor j from location i (all the neighboring hexagons in the moving window were given an equal weight of 1)

n = number of samples in the dataset (the 9,644 hexagons containing tree cover)

W_i^* = the sum of the weights

$s^*_1 i$ = the number of samples within d of the central location (19: the focal hexagon and its 18 first- and second-order neighbors)

$\bar{x}^*$ = the mean of whole dataset (in this case, for all 9,644 hexagons containing tree cover)

s^* = the standard deviation of whole dataset (for all 9,644 hexagons containing tree cover)

G_i^* is standardized as a z-score with a mean of 0 and a standard deviation of 1, with values >1.96 representing significant local clustering of higher fire occurrence densities (p <0.025) and values <-1.96 representing significant clustering of lower fire occurrence densities (p <0.025), because 95 percent of the observations under a normal distribution should be within approximately two standard deviations of the mean (Laffan 2006). Values between -1.96 and 1.96 have no statistically significant concentration of high or low values; a hexagon and its 18 neighbors, in other words, have a normal range of both high and low numbers of fire occurrences/100 km^2 of tree canopy cover area. It is worth noting that the threshold values are not exact because the correlation of spatial data violates the assumption of independence required for statistical significance (Laffan 2006). In addition, the Getis-Ord approach does not require that the input data be normally distributed, because the local G_i^* values are computed under a randomization assumption, with G_i^* equating to a standardized z-score that asymptotically tends to a normal distribution (Anselin 1992). The z-scores are considered to be reliable, even with skewed data, as long as the local neighborhood encompasses several observations (ESRI 2017), in this case, via the target hexagon and its 18 first- and second-order neighbors.

RESULTS AND DISCUSSION

Trends in Forest Fire Occurrence Detections for 2019

The MODIS Active Fire database recorded 40,657 forest fire occurrences across the conterminous United States in 2019, the fifth lowest in 19 full years of data collection and the least in a year since 2005 (fig. 3.1). This was a decline of approximately 47 percent from 2018 (76,692 total forest fire occurrences), and 43 percent lower than the mean of the previous 18 years of data. At the same time, Alaska experienced a dramatic 3,740-percent increase in fire occurrences from 2018, from 690 to 26,493, as well as a 157-percent increase over the mean of the previous years. This was the third most fire occurrences in Alaska in 19 years of data collection, and the most since 2005. Hawaii had only 36 fire occurrences in 2019, which was a 74-percent drop from 2018 (136) and an 88-percent decrease from the 2001–2018 average. Finally, 18 fire occurrences were detected in Puerto Rico, an increase from the single occurrence in 2018 and about 85 percent above the average of 9.7 per year.

The decrease in fire occurrences in the conterminous United States along with the stark upsurge in fire occurrences in Alaska are in keeping with the official national wildland fire statistics, which are based on numbers of wildfires reported and area burned (National

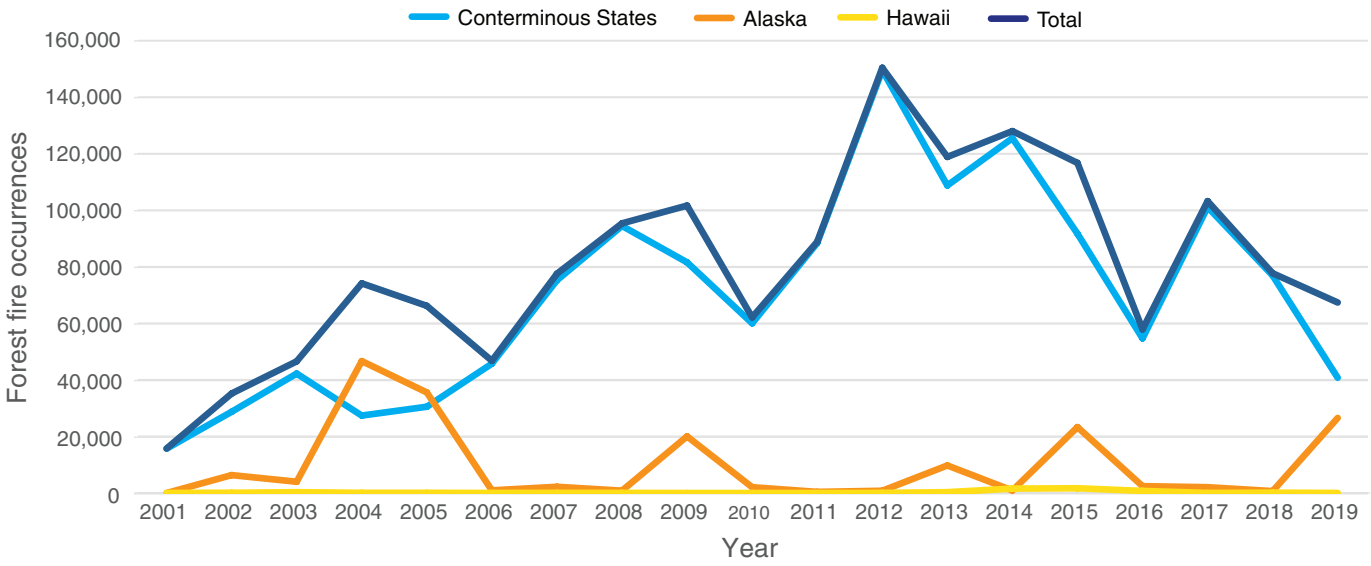

Figure 3.1—Forest fire occurrences detected by Moderate Resolution Imaging Spectroradiometer (MODIS) from 2001 through 2019 for the conterminous United States, Alaska, and Hawaii, and for the entire Nation combined. (Data source: U.S. Department of Agriculture Forest Service, Geospatial Technology and Applications Center, in conjunction with the NASA MODIS Rapid Response group)

Interagency Coordination Center 2020). According to these statistics, there were 50,477 wildfires nationally in 2019 compared to 58,083 in 2018, while the area burned declined 47 percent from 3 548 078 ha in 2018 to 1 887 601 ha in 2019, and was 33 percent less than the 10-year average (National Interagency Coordination Center 2019, 2020). Alaska was the only region in the United States with a larger-than-average area burned as well as the only region with a significant increase in number of fires reported. Across the United States in 2019, the number of wildland fires and fire complexes exceeding 16 187 ha (40,000 acres, a benchmark threshold for the National Interagency Coordination Center) was only 27, compared to 49 in 2018 and 44 in 2017 (National Interagency Coordination Center 2018, 2019, 2020). Of these, all but two of the 15 largest U.S. fires in 2019 occurred in Alaska (National Interagency Coordination Center 2020). As noted in the Methods section above, estimates of burned area and numbers of reported fires are different metrics for quantifying fire activity than calculations of MODIS-detected fire occurrences, though they may be correlated.

This was not the first time that a peak fire year in Alaska corresponded with a decrease in fire occurrences in the conterminous

United States (fig. 3.1). In 2004 and 2005, in fact, the number of fire occurrences in Alaska exceeded those of the conterminous States, the only times during the MODIS period that this happened. Additionally, peaks of Alaska fire occurrences in 2009 and 2015 were followed the next year by a marked decrease in conterminous States fire occurrences. Such broad-scale patterns of wildfire throughout North America are the result of the interaction between climate and vegetation development across a range of spatial and temporal scales, with climate influencing fine fuel moisture, ignition frequency, and rates of wildfire spread at annual to interannual timescales (Gedalof 2011) and with years of high fire activity in the West characterized by widespread and regionally distinct summer droughts (Trouet and others 2010). Interannual to multidecadal variability in sea surface temperatures, associated with the El Niño-Southern Oscillation (ENSO), Pacific Decadal Oscillation (PDO), and Atlantic Multidecadal Oscillation (AMO), drive intermediate-term patterns in wildfire occurrence in North America (Kitzberger and others 2007). Further research could help illuminate the relationships between climate and wildfire occurrences within and between regions of the conterminous 48 States and Alaska.

Areas with the highest fire occurrence densities in 2019 were in southwestern Idaho, central California, and eastern Kansas (fig. 3.2). The Owyhee Uplands (342C) was the ecoregion section with the highest fire occurrence density in 2019, with 8.8 fire occurrences/100 km^2 of tree canopy cover (table 3.1). (In the previous year, the ecoregion section with the highest fire occurrence density was the Northern California Coast Ranges [M261B], which experienced 31.8 fire occurrences/100 km^2 of tree canopy cover [Potter 2020a]). Two other ecoregion sections had relatively high fire occurrence densities: 262A–Great Valley in California (8.4 fire occurrences/100 km^2 of tree canopy cover) and 251F–Flint Hills in Kansas (6.7 fire occurrences/100 km^2 of tree canopy cover). A handful of ecoregion sections in the Southeast, in Arizona and New Mexico, in northern California, and in Oregon and Washington had moderate fire occurrence densities (fig. 3.2). The relatively low fire occurrence densities across the conterminous 48 States were attributable at least in part to the atypical summer of 2019, during which spring-like temperatures held until early July, and long-duration and hot high-pressure ridge events did not develop in the West (National Interagency Coordination Center 2020).

On the other hand, Alaska experienced extraordinarily hot and dry conditions in June and July, with July 2019 being the hottest month on record for the State; conditions were critically dry in the interior as the summer rains arrived later than usual in August and missed the south-central part of Alaska (National Interagency Coordination Center 2020). As a result, fire occurrence densities across large swaths of central and south-central Alaska were moderate, with densities very high in 132A–Yukon-Old Crow Basin (19.4 fire occurrences/100 km^2 of forest and shrub cover) (fig. 3.3). This ecoregion section

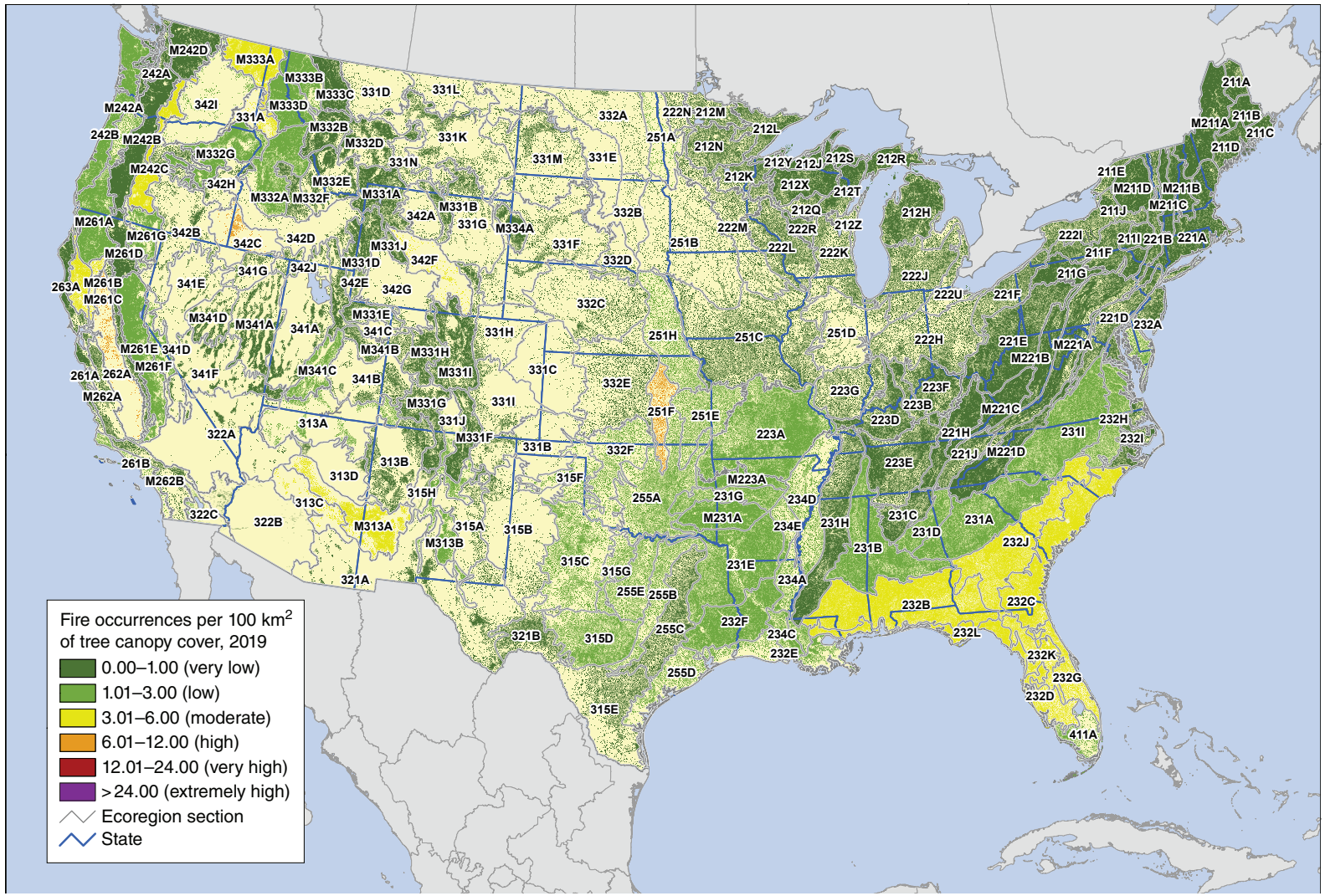

Figure 3.2—The number of forest fire occurrences, per 100 km^2 (10 000 ha) of tree canopy coverage area, by ecoregion section within the conterminous 48 States, for 2019. The gray lines delineate ecoregion sections (Cleland and others 2007). Tree canopy cover is based on data from a cooperative project between the Multi-Resolution Land Characteristics Consortium (Coulston and others 2012) and the Forest Service Geospatial Technology and Applications Center using the 2011 National Land Cover Database. See figure 1.1A for ecoregion identification. (Source of fire data: U.S. Department of Agriculture Forest Service, Geospatial Technology and Applications Center, in conjunction with the NASA MODIS Rapid Response group)

Table 3.1—The 15 ecoregion sections in the conterminous United States with the highest fire occurrence densities in 2019

Section	Name	Tree canopy area	Fire occurrences	Density[a]
		km²	*number*	
342C	Owyhee Uplands	16.7	148	8.8
262A	Great Valley	19.4	164	8.4
251F	Flint Hills	57.8	387	6.7
232B	Gulf Coastal Plains and Flatwoods	888.7	4770	5.4
232J	Southern Atlantic Coastal Plains and Flatwoods	604.0	2,865	4.7
342F	Central Basin and Hills	16.5	77	4.7
232K	Florida Coastal Plains Central Highlands	149.0	632	4.2
M261C	Northern California Interior Coast Ranges	18.2	73	4.0
M261B	Northern California Coast Ranges	114.1	439	3.8
M333A	Okanogan Highland	247.9	919	3.7
232D	Florida Coastal Lowlands-Gulf	134.9	491	3.6
M313A	White Mountains-San Francisco Peaks-Mogollon Rim	202.5	717	3.5
232G	Florida Coastal Lowlands-Atlantic	138.5	471	3.4
331A	Palouse Prairie	33.4	107	3.2
313C	Tonto Transition	17.5	55	3.2

[a] Density = fire occurrences/100 km^2 of tree canopy coverage area.

was the location of the Chalkyitsik Complex of fires, which burned 204 463 ha and cost approximately $7 million to contain (National Interagency Coordination Center 2020).

In Hawaii, only a single area had at least moderate fire occurrence density in 2019, the Lowland/Leeward Dry ecoregion on Maui island (LLDm) with fire occurrence density of 5.5/100 km^2 of tree canopy cover (fig. 3.4).

All other ecoregions in the State had 2019 fire occurrence densities of ≤3/100 km^2 of tree canopy cover. This followed a year during which a dramatic Big Island lava eruption in the lower east rift zone of the Kīlauea volcano burned forests and homes at the very eastern tip of the island (Andrews 2018), resulting in a high fire occurrence density (7.4/100 km^2 of tree canopy cover) in the island's Lowland Wet-Hilo-Puna ecoregion (LWh-hp) (Potter 2020a).

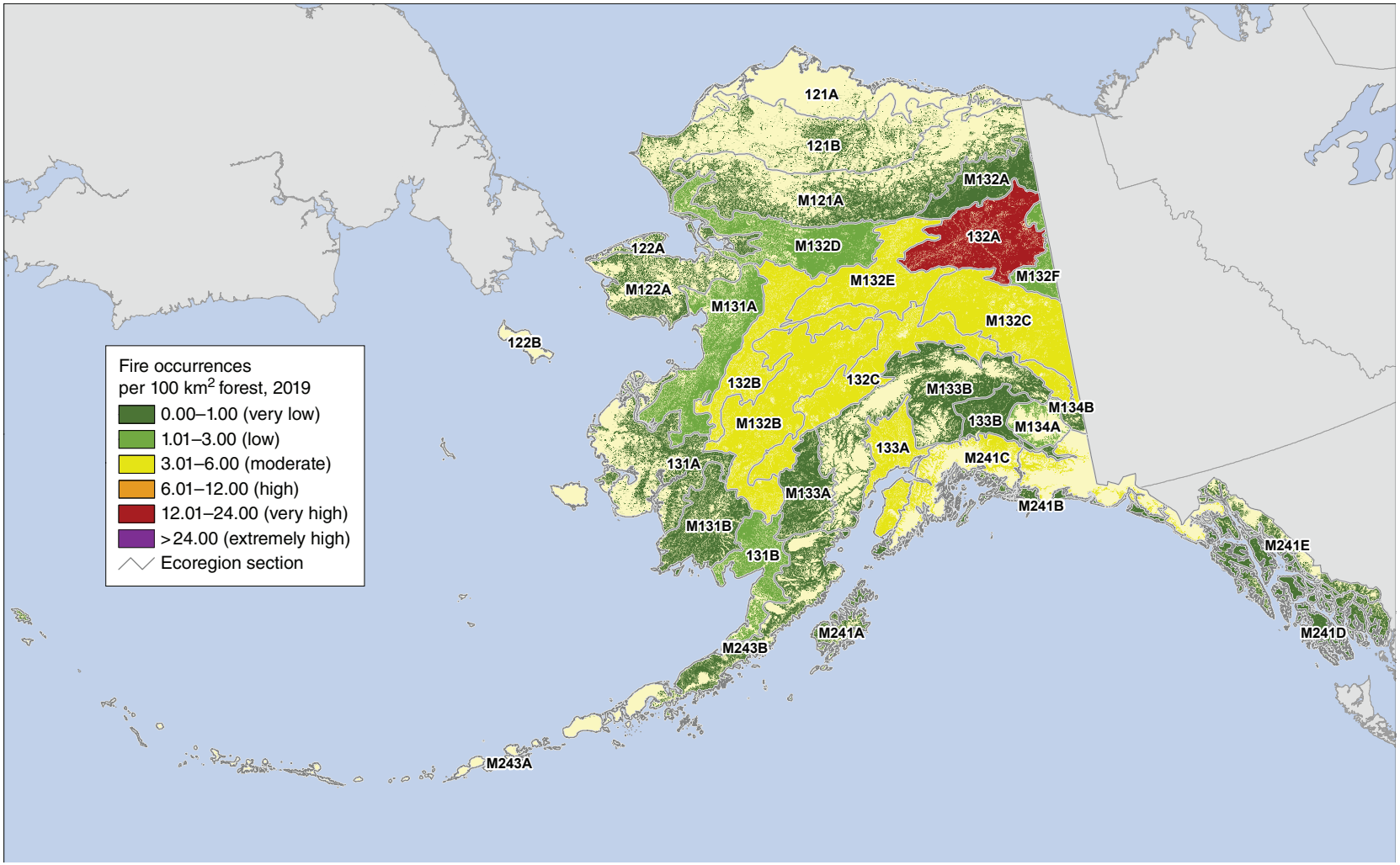

Figure 3.3—The number of forest fire occurrences, per 100 km^2 (10 000 ha) of forest and shrub cover, by ecoregion section within Alaska, for 2019. The gray lines delineate ecoregion sections (Spencer and others 2002). Forest and shrub cover are derived from the 2011 National Land Cover Database. See figure 1.1B for ecoregion identification. (Source of fire data: U.S. Department of Agriculture Forest Service, Geospatial Technology and Applications Center, in conjunction with the NASA MODIS Rapid Response group)

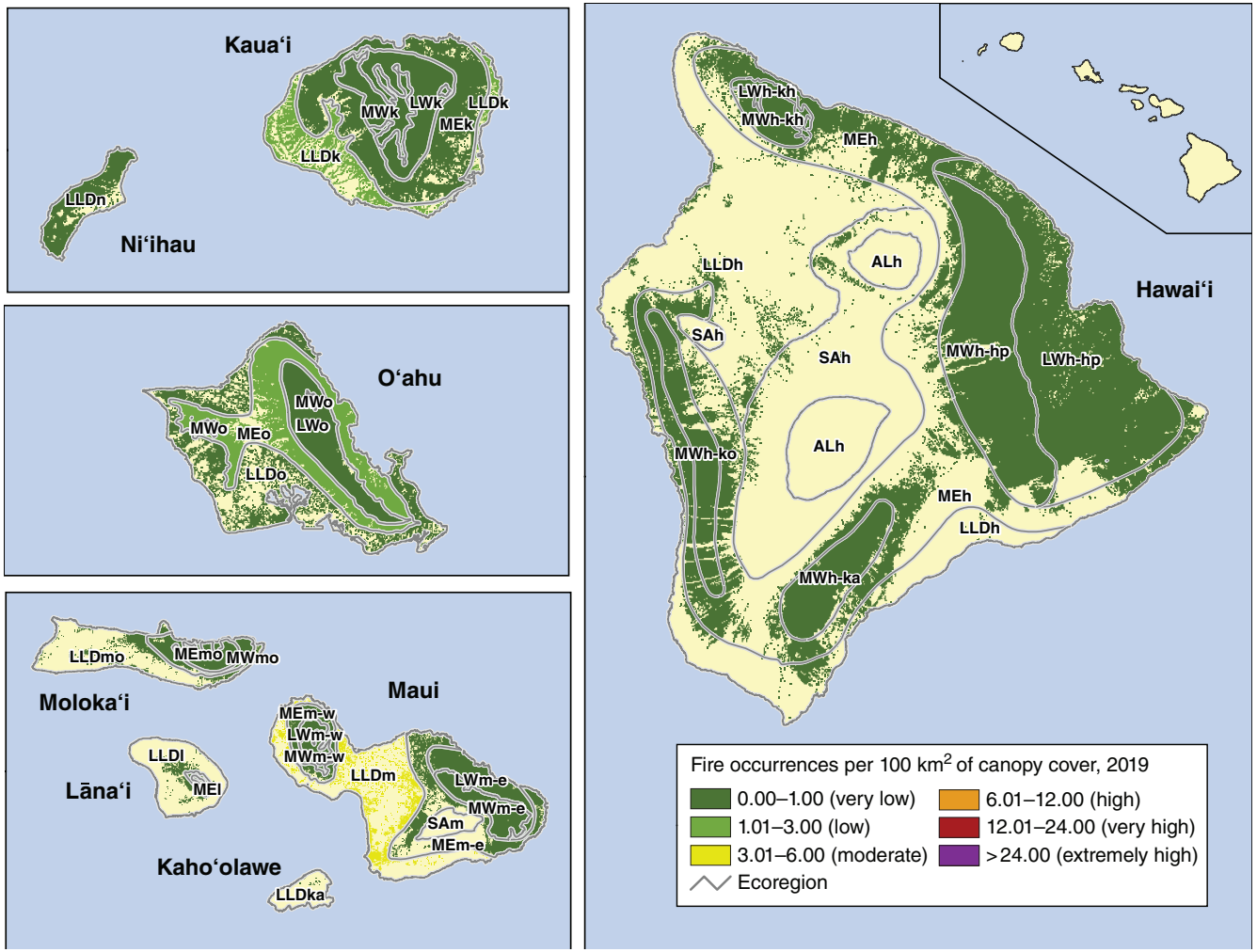

Figure 3.4—The number of forest fire occurrences, per 100 km^2 (10 000 ha) of tree canopy coverage area, by island/ecoregion combination in Hawaii, for 2019. Tree canopy cover is based on data from a cooperative project between the Multi-Resolution Land Characteristics Consortium (Coulston and others 2012) and the Forest Service Geospatial Technology and Applications Center using the 2011 National Land Cover Database. See table 1.1 for ecoregion identification. (Source of fire data: U.S. Department of Agriculture Forest Service, Geospatial Technology and Applications Center, in conjunction with the NASA MODIS Rapid Response group)

Finally, 2019 fire occurrence densities were ≤1/100 km^2 of tree canopy cover for all of the islands of the U.S. Caribbean territories (Puerto Rico and the U.S. Virgin Islands) (fig. 3.5).

Comparison to Longer Term Trends

The nature of the MODIS Active Fire data makes it possible to contrast short-term (2019) forest fire occurrence densities with longer term trends encompassing the first 18 full years of data collection (2001–2018) for ecoregions in the conterminous States, Alaska, and Hawaii, and for Caribbean islands. Across that multiyear period, the highest mean annual fire occurrences in the conterminous States are in ecoregion sections of the northern Rocky Mountains, California, the Southwest, the southern Great Plains, and the Southeastern Coastal Plain (fig. 3.6A). Meanwhile, ecoregions elsewhere generally experienced ≤3 fire occurrences/100 km^2 of tree canopy cover annually, with the Northeast and most of the Midwest having ≤1. The M332A–Idaho Batholith in central Idaho had the highest fire occurrence density on average (mean annual fire occurrence density of 12.8), followed by M261A–Klamath Mountains of northwestern California and southeastern Oregon (10.6) (table 3.2). Other ecoregion sections with high mean fire occurrence densities (6.01–12.00 fire occurrences/100 km^2 of canopy cover) were located along the Gulf Coast in the Southeast; in coastal, northern, and central areas of California; in north-central Washington; in central Arizona and New Mexico; in the northern Rocky Mountains; and in central Kansas and northeastern Oklahoma (table 3.2). The ecoregion section with the greatest annual variation in fire occurrence densities from 2001 to 2018 was again M332A–Idaho Batholith, with more moderate variation in California, northeastern Washington and northwestern Idaho, southern Oregon, western Montana, and central Arizona and west-central New Mexico (fig. 3.6B). The Northeast and most of the Midwest had the lowest variation, while relatively low variation was also present across the Southeast, the central Rocky Mountain States, the Great Basin, and central Oregon and Washington.

Most of the conterminous United States experienced near-normal fire occurrence densities in 2019, compared to the previous 17-year mean and accounting for variability over time (fig. 3.6C). As determined by the calculation of standardized fire occurrence *z*-scores, a few ecoregions in the Northeast and scattered elsewhere had significantly higher fire occurrence densities than normal. The ecoregion section with the highest *z*-score in 2019 was 212J–Southern Superior Uplands, an area with typically very few fire occurrences. Other similar ecoregion sections were 211A–Aroostook Hills and Lowlands of northern Maine, 221A–Lower New England along the Atlantic Coast from New York to Maine, 342C–Southern Superior Uplands in southwest Idaho, 315B–Texas High Plains in western Texas and eastern New Mexico, 331J–Northern Rio Grande Basin in north-central New Mexico and south-central Colorado, and 262A–Great Valley in central California.

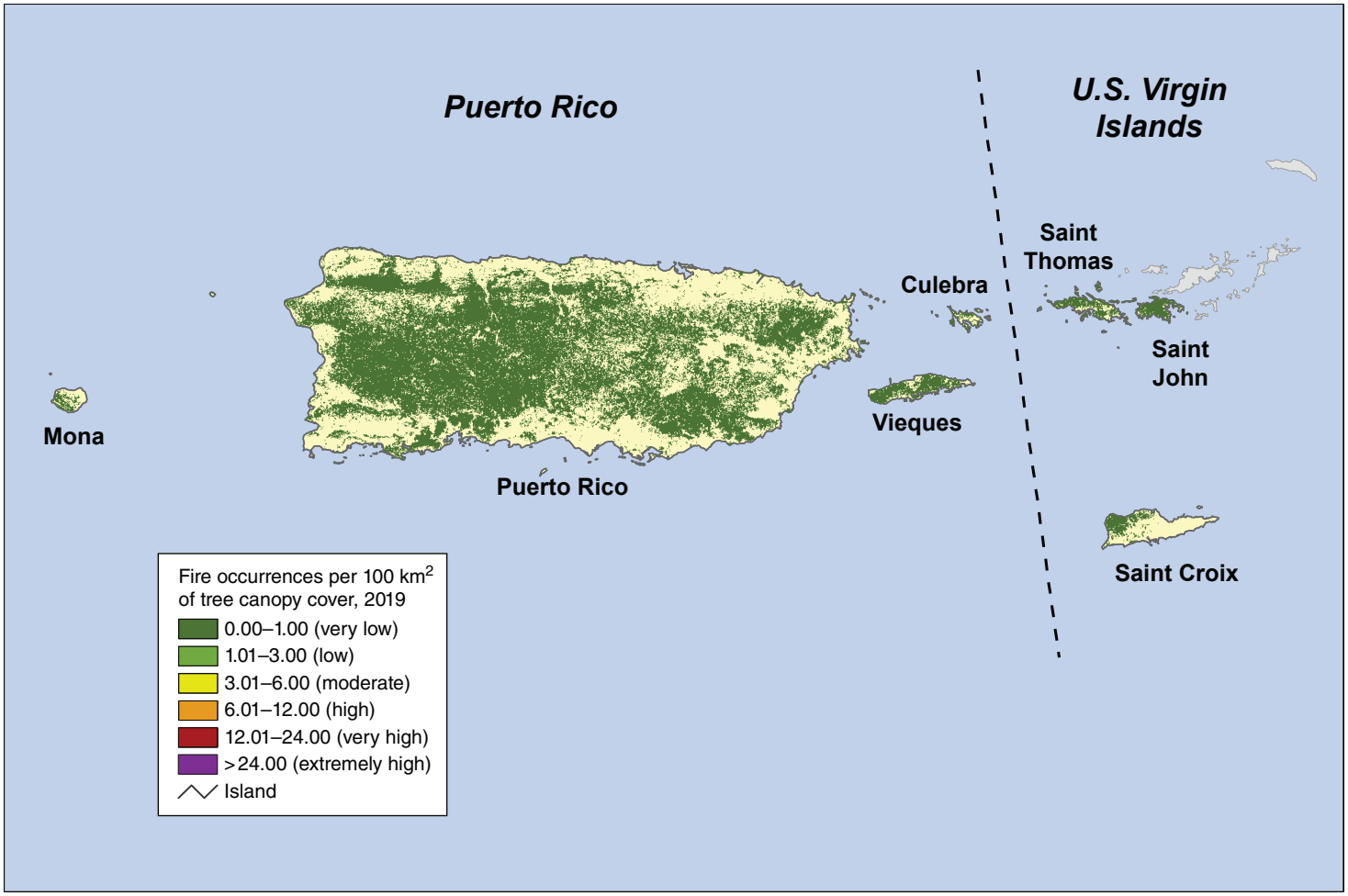

Figure 3.5—The number of forest fire occurrences, per 100 km^2 (10 000 ha) of tree canopy coverage area, by island in Puerto Rico and the U.S. Virgin Islands, for 2019. Tree canopy cover is based on data from a cooperative project between the Multi-Resolution Land Characteristics Consortium (Coulston and others 2012) and the Forest Service Geospatial Technology and Applications Center using the 2011 National Land Cover Database. (Source of fire data: U.S. Department of Agriculture Forest Service, Geospatial Technology and Applications Center, in conjunction with the NASA MODIS Rapid Response group)

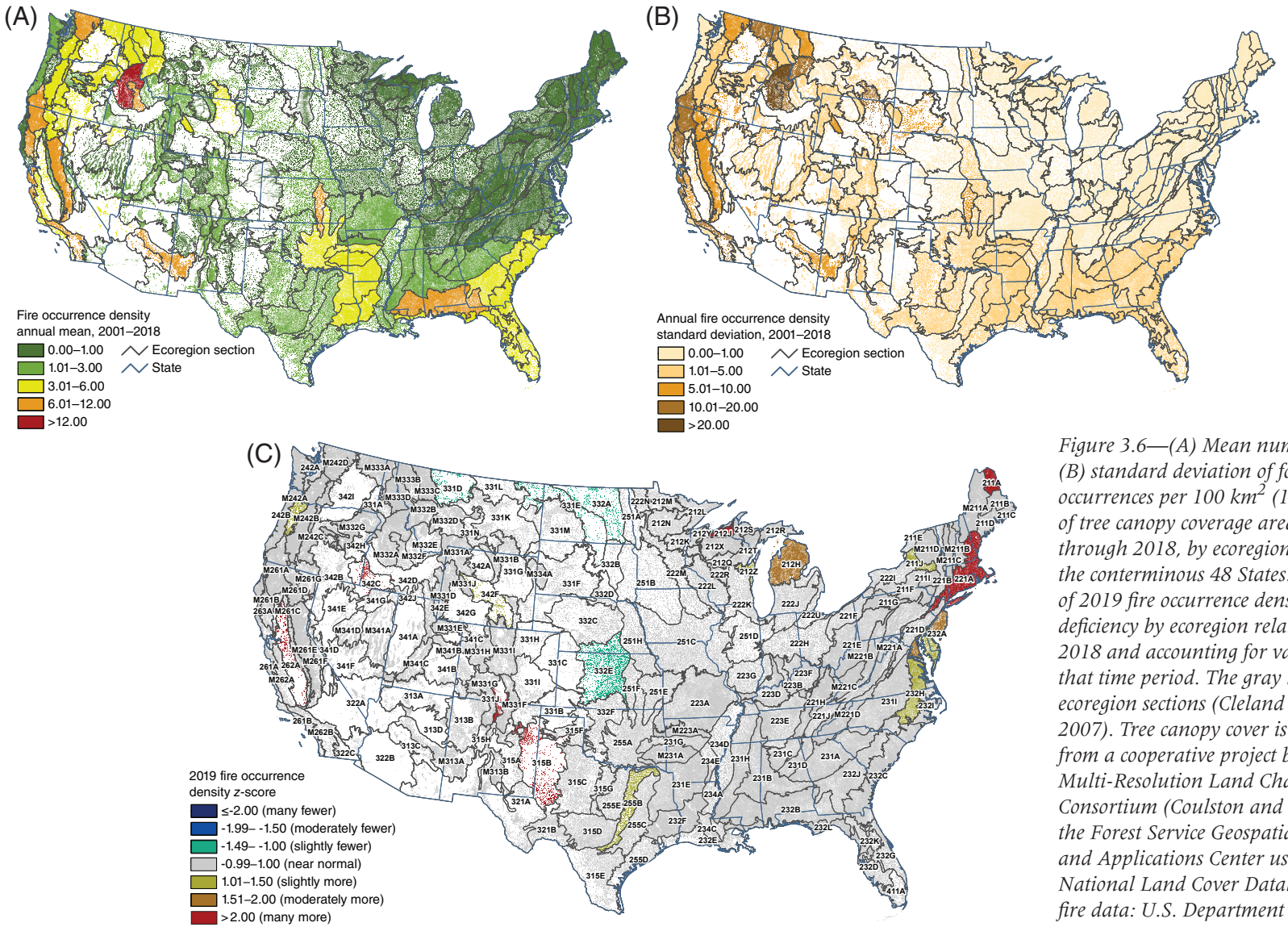

Figure 3.6—(A) Mean number and (B) standard deviation of forest fire occurrences per 100 km^2 (10 000 ha) of tree canopy coverage area from 2001 through 2018, by ecoregion section within the conterminous 48 States. (C) Degree of 2019 fire occurrence density excess or deficiency by ecoregion relative to 2001–2018 and accounting for variation over that time period. The gray lines delineate ecoregion sections (Cleland and others 2007). Tree canopy cover is based on data from a cooperative project between the Multi-Resolution Land Characteristics Consortium (Coulston and others 2012) and the Forest Service Geospatial Technology and Applications Center using the 2011 National Land Cover Database. (Source of fire data: U.S. Department of Agriculture Forest Service, Geospatial Technology and Applications Center, in conjunction with the NASA MODIS Rapid Response group)

Table 3.2—The 15 ecoregion sections in the conterminous United States with the highest mean annual fire occurrence densities from 2001 to 2018

Section	Name	Tree canopy area	Mean annual fire occurrence density[a]
		km^2	
M332A	Idaho Batholith	338.9	12.8
M261A	Klamath Mountains	338.5	10.6
M262B	Southern California Mountain and Valley	58.1	8.8
M261E	Sierra Nevada	427.8	7.9
M313A	White Mountains-San Francisco Peaks-Mogollon Rim	202.5	7.7
313C	Tonto Transition	17.5	7.5
251F	Flint Hills	57.8	6.9
M261B	Northern California Coast Ranges	114.1	6.7
M242D	Northern Cascades	251.1	6.7
261A	Central California Coast	66.8	6.3
232B	Gulf Coastal Plains and Flatwoods	888.7	6.1
M332F	Challis Volcanics	72.2	6.1
M333C	Northern Rockies	176.3	5.9
331A	Palouse Prairie	33.4	5.8
M332B	Northern Rockies and Bitterroot Valley	154.9	5.7

[a] Mean annual fire occurrence density = fire occurrences/100 km^2 of tree canopy coverage area.

A few ecoregion sections in the middle part of the country had 2019 fire occurrence densities that were lower than the longer term as indicated by *z*-scores that were ≤-1: 331E–Northeastern Glaciated Plains in central and northwest North Dakota and northeastern Montana; 332E–South-Central Great Plains in central Kansas and south-central Nebraska; 332A–Northeastern Glaciated Plains in central North Dakota; and 331D–Northwestern Glaciated Plains in north-central Montana (fig. 3.6C). Each of these has a relatively low proportion of tree canopy cover, and each had a very low fire occurrence density score in 2019.

In Alaska, meanwhile, the central and east-central parts of the State had moderate mean annual fire occurrence densities for 2001–2018, specifically in 132A–Yukon-Old Crow Basin and M132E–Ray Mountains (fig. 3.7A). These ecoregion sections, along with M132C–Yukon-Tanana Uplands and M132F–North Ogilvie Mountains, were the most variable over the

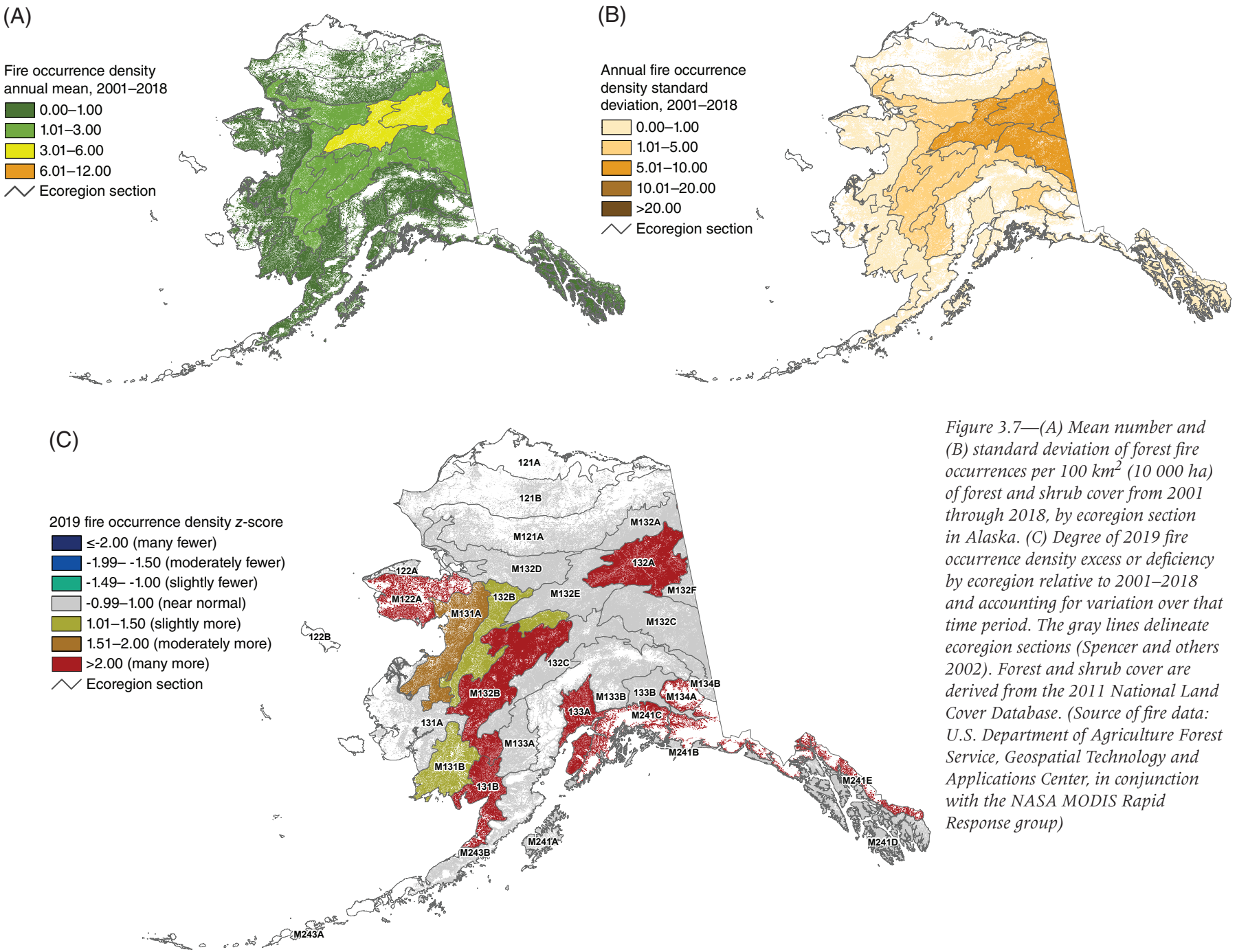

Figure 3.7—(A) Mean number and (B) standard deviation of forest fire occurrences per 100 km^2 (10 000 ha) of forest and shrub cover from 2001 through 2018, by ecoregion section in Alaska. (C) Degree of 2019 fire occurrence density excess or deficiency by ecoregion relative to 2001–2018 and accounting for variation over that time period. The gray lines delineate ecoregion sections (Spencer and others 2002). Forest and shrub cover are derived from the 2011 National Land Cover Database. (Source of fire data: U.S. Department of Agriculture Forest Service, Geospatial Technology and Applications Center, in conjunction with the NASA MODIS Rapid Response group)

18-year period preceding 2019 (fig. 3.7B). In 2019, much of the State had higher fire occurrence densities compared to the previous 18 years and accounting for variability (fig. 3.7C). The ecoregion sections that had many more fire occurrence densities than expected were 132A–Yukon-Old Crow Basin in the east; M122A–Seward Peninsula in the west; M132B–Kuskokwim Mountains and 131B–Bristol Bay Lowlands in the southwest; 133A–Cook Inset Basin, M241C–Chugach-St. Elias Mountains, and M134A–Wrangell Mountains in the south-central and southeastern parts of the State; and M241E–Northern Coast Mountains in the panhandle. Other ecoregions in western Alaska had fire occurrence densities that were moderately or slightly higher than expected.

In Hawaii, the Lowland Wet-Hilo-Puna ecoregion (LWh-hp) of the Big Island had both the highest annual fire occurrence density mean (fig. 3.8A) and variability (fig. 3.8B) during the 2001–2018 period. The annual mean was ≤1 fire occurrence/100 km^2 of tree cover for all other ecoregions with the exception of the Mesic region on the Big Island (MEh), which was 2.7. In 2019, ecoregions on three other islands had fire occurrence densities higher than expected, controlling for variability over the previous 18 years (z-score >1). Three ecoregions had many more fire occurrences than expected: Lowland/Leeward Dry ecoregion on Maui (LLDm), Mesic on O‘ahu (MEo), and Lowland/Leeward Dry on Kaua‘i (LLDk) (fig. 3.7C). An additional ecoregion had moderately more fire occurrences than expected: Lowland Wet on O‘ahu (LWo).

Finally, the 2001–2018 fire occurrence means and standard deviations were ≤1 for all the islands of the Caribbean territories of Puerto Rico and the U.S. Virgin Islands (figs. 3.9A and 3.9B). Only Puerto Rico was outside the range of near-normal fire occurrence density (z-score ≤-1 or >1) in 2019, having moderately more fire occurrences than expected (fig. 3.9C).

Geographical Hot Spots of Fire Occurrence Density

The results presented thus far summarize the 2019 fire occurrence data at the ecoregion scale (or by island in the Caribbean territories). Geographic hot spot analyses, conducted across the conterminous United States using analysis units smaller than ecoregions, can offer additional insights into where, statistically, fire occurrences are more concentrated than expected by chance. As noted above, the 2019 wildfire season was relatively mild in the conterminous States compared to recent years. The hot spot analysis, however, is limited to a single year and therefore identifies areas that have higher-than-expected fire occurrence densities in 2019 compared to the entire study region. For 2019, the SASH method detected two geographic hot spots of very high fire occurrence density (G_i* >12 and ≤24) as well as several hot spots of high density (G_i* >6 and ≤12) (fig. 3.10).

The hot spots of very high fire occurrence density were in southern Arizona (322B–Sonoran Desert and 321A–Basin and Range) and in southeastern Georgia (232B–Gulf Coastal Plains and Flatwoods). Hot spots of

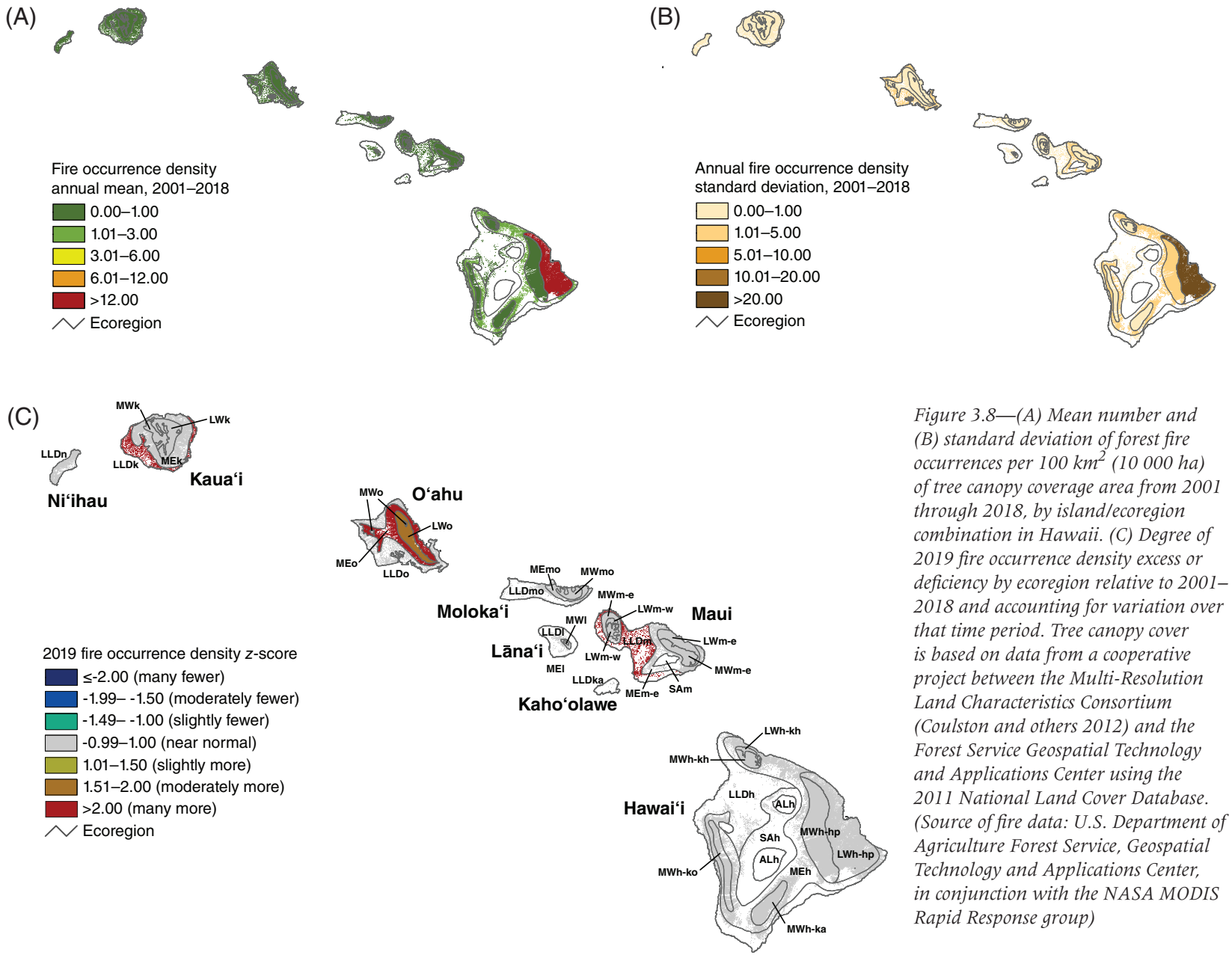

Figure 3.8—(A) Mean number and (B) standard deviation of forest fire occurrences per 100 km^2 (10 000 ha) of tree canopy coverage area from 2001 through 2018, by island/ecoregion combination in Hawaii. (C) Degree of 2019 fire occurrence density excess or deficiency by ecoregion relative to 2001–2018 and accounting for variation over that time period. Tree canopy cover is based on data from a cooperative project between the Multi-Resolution Land Characteristics Consortium (Coulston and others 2012) and the Forest Service Geospatial Technology and Applications Center using the 2011 National Land Cover Database. (Source of fire data: U.S. Department of Agriculture Forest Service, Geospatial Technology and Applications Center, in conjunction with the NASA MODIS Rapid Response group)

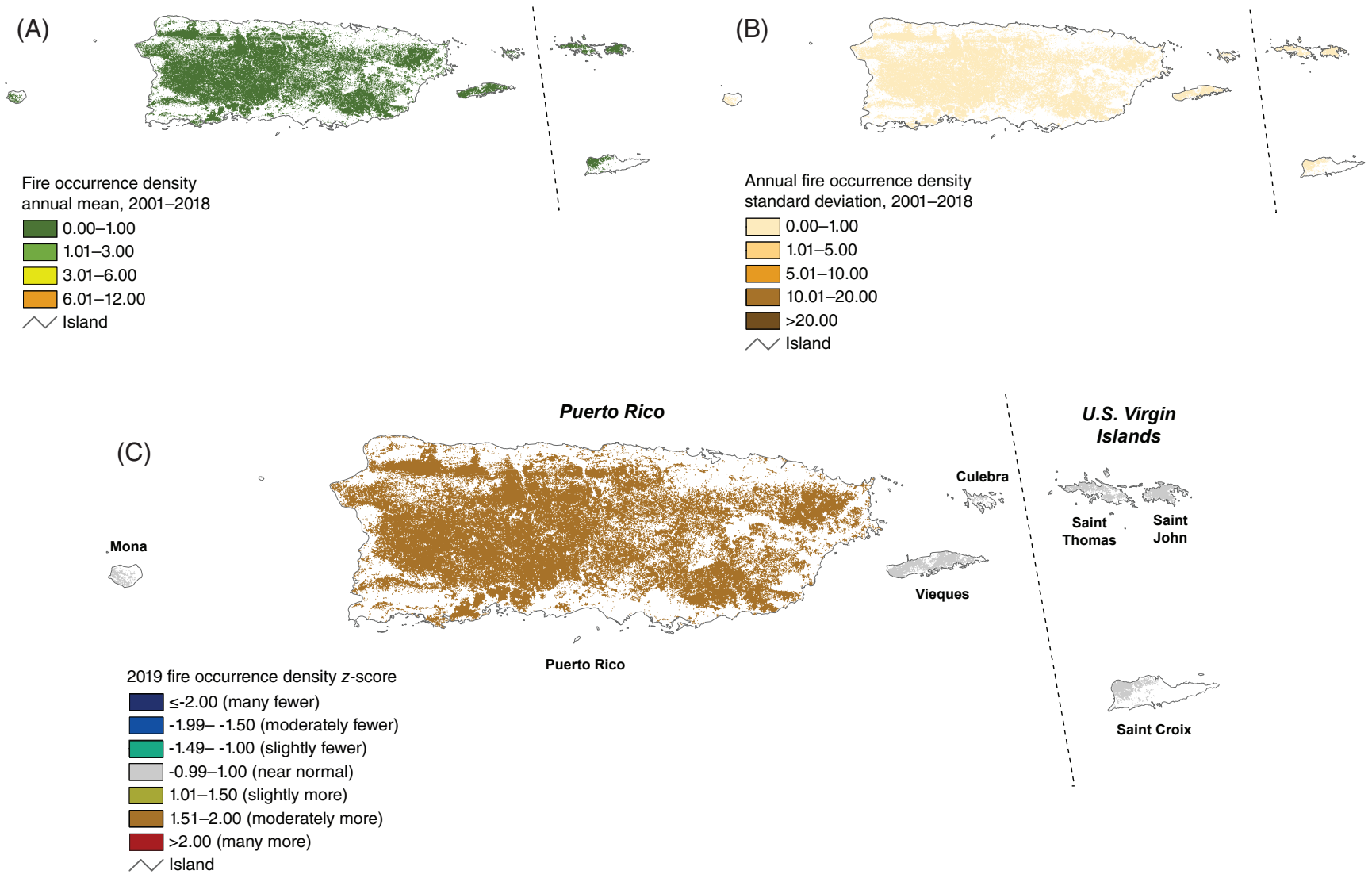

Figure 3.9—(A) Mean number and (B) standard deviation of forest fire occurrences per 100 km^2 (10 000 ha) of forested area from 2001 through 2018, by island in Puerto Rico and the U.S. Virgin Islands. (C) Degree of 2019 fire occurrence density excess or deficiency by ecoregion relative to 2001–2018 and accounting for variation over that time period. Tree canopy cover is based on data from a cooperative project between the Multi-Resolution Land Characteristics Consortium (Coulston and others 2012) and the U.S. Department of Agriculture Forest Service, Geospatial Technology and Applications Center using the 2011 National Land Cover Database.

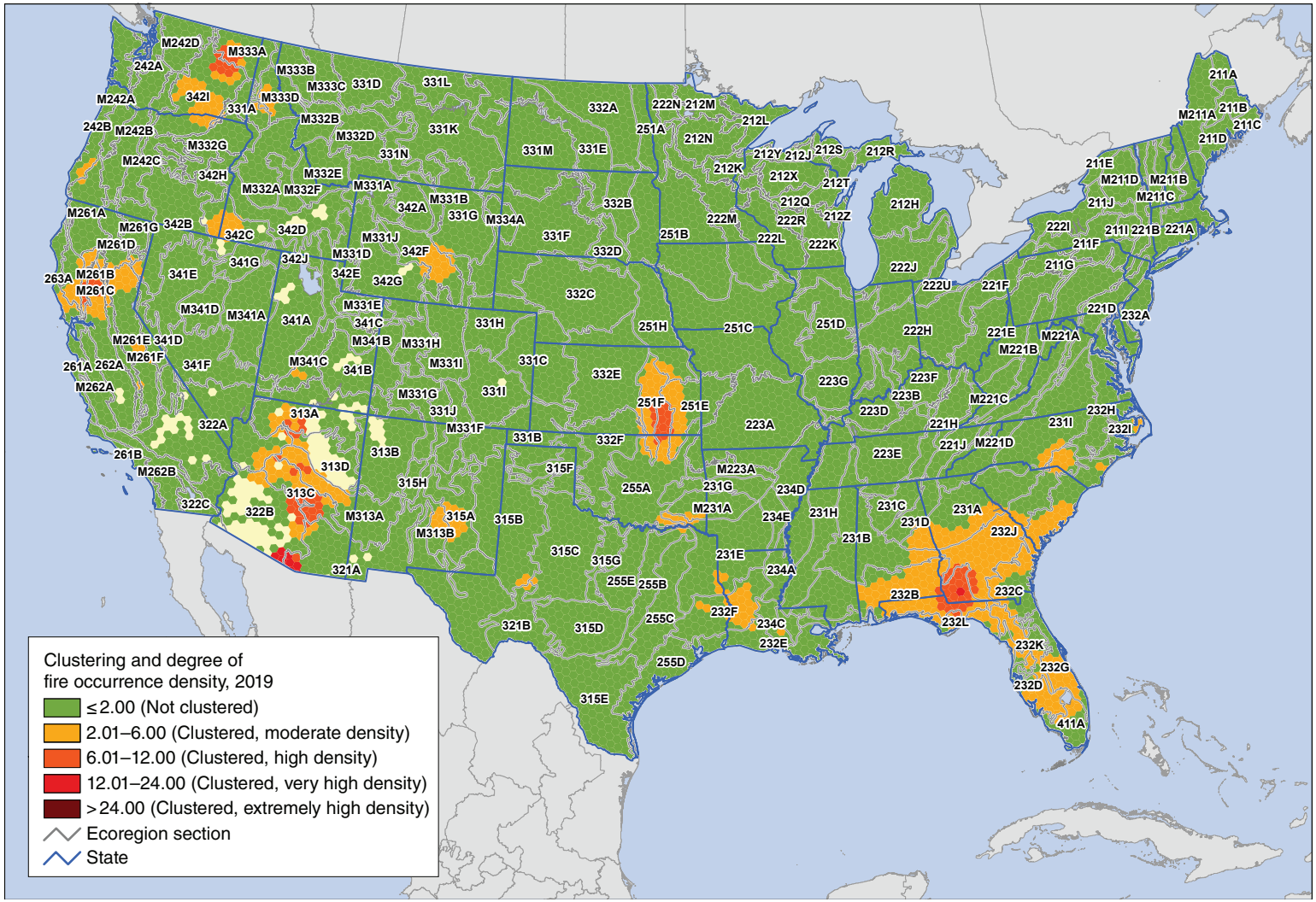

Figure 3.10—Hot spots of fire occurrence across the conterminous United States for 2019. Values are Getis-Ord G_i^* scores, with values >2 representing significant clustering of high fire occurrence densities. (No areas of significant clustering of lower fire occurrence densities, <-2, were detected). The gray lines delineate ecoregion sections (Cleland and others 2007). Background tree canopy cover is based on data from a cooperative project between the Multi-Resolution Land Characteristics Consortium (Coulston and others 2012) and the Forest Service Geospatial Technology and Applications Center using the 2011 National Land Cover Database. (Source of fire data: U.S. Department of Agriculture Forest Service, Geospatial Technology and Applications Center, in conjunction with the NASA MODIS Rapid Response group)

high fire occurrence density were detected in eastern Kansas (255A–Cross Timbers and Prairie and 251F–Flint Hills), northeastern Washington (M333A–Okanogan Highland and 342I–Columbia Basin), north-central California (262A–Great Valley and M261C–Northern California Interior Coast Ranges), northern Arizona (313A–Grand Canyon and 313D–Painted Desert), and central Arizona (M313A–White Mountains-San Francisco Peaks-Mogollon Rim, 313C–Tonto Transition, and 322B–Sonoran Desert) (fig. 3.10).

Hot spots of moderate fire density in 2019 (G_i^* >2 and ≤6) were identified in scattered locations in the Pacific Coast States, the Rocky Mountain States, and the Southeast (fig. 3.10). From west to east, these were detected in:

- Southwestern Oregon (M242A–Oregon and Washington Coast Ranges)
- East-central California (M261E–Sierra Nevada)
- South-central Washington (342I–Columbia Basin)
- Southeastern Oregon and southwestern Idaho (342C–Owyhee Uplands)
- Northern Idaho (M333D–Bitterroot Mountains)
- South-central Utah (M341C–Utah High Plateau)
- South-central Wyoming (342F–Central Basin and Hills)
- Southeastern New Mexico (M313B–Sacramento-Monzano Mountains and 315A–Pecos Valley)
- West-central Texas (315B–Texas High Plains, 315C–Rolling Plains, and 321B–Stockton Plateau)
- Southeastern Kansas and northeastern Oklahoma (251F–Flint Hills, 255A–Cross Timbers and Prairie, and 251E–Osage Plains)
- Southeastern Oklahoma (M231A–Ouachita Mountains, 231E–Mid Coastal Plains-Western, and 255A–Cross Timbers and Prairie)
- Eastern Texas and west-central Louisiana (234C–Atchafalaya and Red River Alluvial Plains)
- South-central Louisiana (232F–Coastal Plains and Flatwoods-Western Gulf and 231E–Mid Coastal Plains-Western)
- Southeastern Alabama, southern and central Georgia, southern South Carolina, and Florida panhandle (232B–Gulf Coastal Plains and Flatwoods, 232J–Southern Atlantic Coastal Plains and Flatwoods, 231A–Southern Appalachian Piedmont, 232C–Atlantic Coastal Flatwoods, and 232L–Gulf Coastal Lowlands)
- Central and southern Florida (232K–Florida Coastal Plains Central Highlands, 232D–Florida Coastal Lowlands-Gulf, 232G–Florida Coastal Lowlands-Atlantic, and 411A–Everglades)
- South-central North Carolina (231I–Central Appalachian Piedmont and 232J–Southern Atlantic Coastal Plains and Flatwoods)
- Southeastern North Carolina (232C–Atlantic Coastal Flatwoods)
- Eastern North Carolina (232I–Northern Atlantic Coastal Flatwoods)

CONCLUSIONS

In 2019, the number of MODIS satellite-detected forest fire occurrences recorded for the conterminous States was uncharacteristically small compared to recent years: the fifth fewest in 19 full years of data collection and the least since 2005. Alaska, however, experienced a particularly severe fire season, with the most fire occurrences since 2005. The relatively low densities of fire occurrences in the conterminous 48 States were attributable at least in part to mild conditions in the early summer, while Alaska experienced extremely hot and dry conditions in June and July.

Ecoregions in southwestern Idaho, central California, and eastern Kansas had the highest forest fire occurrence densities. Geographic hot spots of very high fire occurrence density were detected in southern Arizona and southeast Georgia. Most of the conterminous United States experienced near-normal fire occurrence densities in 2019, compared to the previous 18-year mean and accounting for variability over time, although a few ecoregions in the Northeast and scattered elsewhere had significantly higher fire occurrence densities than normal. Meanwhile, much of Alaska had much higher fire occurrence densities than normal. In Hawaii, ecoregions in Maui, Oʻahu, and Kauaʻi had many more fire occurrences than expected. In the Caribbean, the island of Puerto Rico had moderately more fire occurrences than a normal year.

The results of these geographic analyses are intended to offer insights into where fire occurrences have been concentrated spatially in a given year and compared to previous years but are not intended to quantify the severity of a given fire season. Given the limits of MODIS active fire detection using 1-km-resolution data, these products also may underrepresent the number of fire occurrences in some ecosystems where small and low-intensity fires are common, and where high cloud frequency can interfere with fire detection. These products can also have commission errors. However, these high-temporal-fidelity products currently offer the best means for daily monitoring of forest fire occurrences.

Ecological and forest health impacts relating to fire and other abiotic disturbances are scale-dependent properties, which in turn are affected by management objectives (Lundquist and others 2011). Information about the concentration of fire occurrences may help pinpoint areas of concern for aiding management activities and for investigations into the ecological and socioeconomic impacts of forest fire potentially outside the range of historic frequency.

LITERATURE CITED

Andrews, R.G. 2018. America's most hazardous volcano erupted this year. Then it erupted and erupted. The New York Times. December 12. https://www.nytimes.com/2018/12/12/science/kilauea-hawaii-volcano-eruption.html. [Date accessed: July 15, 2019].

Anselin, L. 1992. Spatial data analysis with GIS: an introduction to application in the social sciences. Tech. Rep. 92-10. Santa Barbara, CA: University of California, National Center for Geographic Information and Analysis. 53 p.

Barbour, M.G.; Burk, J.H.; Pitts, W.D. [and others]. 1999. Terrestrial plant ecology. Menlo Park, CA: Addison Wesley Longman, Inc. 649 p.

Bond, W.J.; Keeley, J.E. 2005. Fire as a global "herbivore": the ecology and evolution of flammable ecosystems. Trends in Ecology & Evolution. 20(7): 387–394. https://doi.org/10.1016/j.tree.2005.04.025.

Cleland, D.T.; Freeouf, J.A.; Keys, J.E. [and others]. 2007. Ecological subregions: sections and subsections for the conterminous United States. Gen. Tech. Rep. WO-76D. Washington, DC: U.S. Department of Agriculture Forest Service. Map; Sloan, A.M., cartographer; presentation scale 1:3,500,000; colored. Also on CD-ROM as a GIS coverage in ArcINFO format or at http://data.fs.usda.gov/geodata/edw/datasets.php. [Date accessed: July 20, 2015].

Coulston, J.W.; Ambrose, M.J.; Riitters, K.H.; Conkling, B.L. 2005. Forest Health Monitoring 2004 national technical report. Gen. Tech. Rep. SRS-90. Asheville, NC: U.S. Department of Agriculture Forest Service, Southern Research Station. 81 p.

Coulston, J.W.; Moisen, G.G.; Wilson, B.T. [and others]. 2012. Modeling percent tree canopy cover: a pilot study. Photogrammetric Engineering and Remote Sensing. 78(7): 715–727. https://doi.org/10.14358/PERS.78.7.715.

Edmonds, R.L.; Agee, J.K.; Gara, R.I. 2011. Forest health and protection. Long Grove, Illinois: Waveland Press, Inc. 667 p.

ESRI. 2017. ArcMap® 10.5.1. Redlands, CA: Environmental Systems Research Institute.

Gedalof, Z. 2011. Climate and spatial patterns of wildfire in North America. In: McKenzie, D.; Miller, C.; Falk, D.A., eds. The landscape ecology of fire. Dordrecht: Springer Netherlands: 89–115. https://doi.org/10.1007/978-94-007-0301-8_4.

Getis, A.; Ord, J.K. 1992. The analysis of spatial association by use of distance statistics. Geographical Analysis. 24(3): 189–206. https://doi.org/10.1111/j.1538-4632.1992.tb00261.x.

Gill, A.M.; Stephens, S.L.; Cary, G.J. 2013. The worldwide "wildfire" problem. Ecological Applications. 23(2): 438–454. https://doi.org/10.1890/10-2213.1.

Hawbaker, T.J.; Radeloff, V.C.; Syphard, A.D. [and others]. 2008. Detection rates of the MODIS active fire product. Remote Sensing of Environment. 112: 2656–2664. https://doi.org/10.1016/j.rse.2007.12.008.

Homer, C.G.; Dewitz, J.A.; Yang, L. [and others]. 2015. Completion of the 2011 National Land Cover Database for the conterminous United States: representing a decade of land cover change information. Photogrammetric Engineering and Remote Sensing. 81(5): 345–354.

Justice, C.O.; Giglio, L.; Korontzi, S. [and others]. 2002. The MODIS fire products. Remote Sensing of Environment. 83(1–2): 244–262. https://doi.org/10.1016/S0034-4257(02)00076-7.

Justice, C.O.; Giglio, L.; Roy, D. [and others]. 2011. MODIS-derived global fire products. In: Ramachandran, B.; Justice, C.O.; Abrams, M.J., eds. Land remote sensing and global environmental change: NASA's earth observing system and the science of ASTER and MODIS. New York: Springer: 661–679. https://doi.org/10.1007/978-1-4419-6749-7_29.

Kitzberger, T.; Brown, P.M.; Heyerdahl, E.K. [and others]. 2007. Contingent Pacific-Atlantic Ocean influence on multicentury wildfire synchrony over western North America. Proceedings of the National Academy of Sciences. 104(2): 543–548. https://doi.org/10.1073/pnas.0606078104.

Laffan, S.W. 2006. Assessing regional scale weed distributions, with an Australian example using *Nassella trichotoma*. Weed Research. 46(3): 194–206. https://doi.org/10.1111/j.1365-3180.2006.00491.x.

Lundquist, J.E.; Camp, A.E.; Tyrrell, M.L. [and others]. 2011. Earth, wind and fire: abiotic factors and the impacts of global environmental change on forest health. In: Castello, J.D.; Teale, S.A., eds. Forest health: an integrated perspective. New York: Cambridge University Press: 195–243. https://doi.org/10.1017/CBO9780511974977.008.

McKenzie, D.; Peterson, D.L.; Alvarado, E. 1996. Predicting the effect of fire on large-scale vegetation patterns in North America. Res. Pap. PNW-489. Portland, OR: U.S. Department of Agriculture Forest Service, Pacific Northwest Research Station. 38 p. https://doi.org/10.5962/bhl.title.87888.

National Interagency Coordination Center. 2018. Wildland fire summary and statistics annual report: 2017. https://www.predictiveservices.nifc.gov/intelligence/2017_statssumm/intro_summary17.pdf. [Date accessed: April 30, 2018].

National Interagency Coordination Center. 2019. Wildland fire summary and statistics annual report: 2018. https://www.predictiveservices.nifc.gov/intelligence/2018_statssumm/intro_summary18.pdf. [Date accessed: June 27, 2019].

National Interagency Coordination Center. 2020. Wildland fire summary and statistics annual report: 2019. https://www.predictiveservices.nifc.gov/intelligence/2019_statssumm/intro_summary19.pdf. [Date accessed: April 3, 2020].

Nowacki, G.J.; Abrams, M.D. 2008. The demise of fire and "mesophication" of forests in the Eastern United States. BioScience. 58(2): 123–138. https://doi.org/10.1641/B580207.

Potter, K.M. 2012a. Large-scale patterns of forest fire occurrence in the conterminous United States and Alaska, 2005–07. In: Potter, K.M.; Conkling, B.L., eds. Forest Health Monitoring 2008 national technical report. Gen. Tech. Rep. SRS-158. Asheville, NC: U.S. Department of Agriculture Forest Service, Southern Research Station: 73–83.

Potter, K.M. 2012b. Large-scale patterns of forest fire occurrence in the conterminous United States and Alaska, 2001–08. In: Potter, K.M.; Conkling, B.L., eds. Forest Health Monitoring 2009 national technical report. Gen. Tech. Rep. SRS-167. Asheville, NC: U.S. Department of Agriculture Forest Service, Southern Research Station: 151–161.

Potter, K.M. 2013a. Large-scale patterns of forest fire occurrence in the conterminous United States and Alaska, 2009. In: Potter, K.M.; Conkling, B.L., eds. Forest Health Monitoring: national status, trends, and analysis 2010. Gen. Tech. Rep. SRS-176. Asheville, NC: U.S. Department of Agriculture Forest Service, Southern Research Station: 31–39.

Potter, K.M. 2013b. Large-scale patterns of forest fire occurrence in the conterminous United States and Alaska, 2010. In: Potter, K.M.; Conkling, B.L., eds. Forest Health Monitoring: national status, trends, and analysis 2011. Gen. Tech. Rep. SRS-185. Asheville, NC: U.S. Department of Agriculture Forest Service, Southern Research Station: 29–40.

Potter, K.M. 2014. Large-scale patterns of forest fire occurrence in the conterminous United States and Alaska, 2011. In: Potter, K.M.; Conkling, B.L., eds. Forest Health Monitoring: national status, trends, and analysis 2012. Gen. Tech. Rep. SRS-198. Asheville, NC: U.S. Department of Agriculture Forest Service, Southern Research Station: 35–48.

Potter, K.M. 2015a. Large-scale patterns of forest fire occurrence in the conterminous United States and Alaska, 2012. In: Potter, K.M.; Conkling, B.L., eds. Forest Health Monitoring: national status, trends, and analysis 2013. Gen. Tech. Rep. SRS-207. Asheville, NC: U.S. Department of Agriculture Forest Service, Southern Research Station: 37–53.

Potter, K.M. 2015b. Large-scale patterns of forest fire occurrence in the conterminous United States and Alaska, 2013. In: Potter, K.M.; Conkling, B.L., eds. Forest Health Monitoring: national status, trends, and analysis 2014. Gen. Tech. Rep. SRS-209. Asheville, NC: U.S. Department of Agriculture Forest Service, Southern Research Station: 39–55.

Potter, K.M. 2016. Large-scale patterns of forest fire occurrence in the conterminous United States, Alaska, and Hawaii, 2014. In: Potter, K.M.; Conkling, B.L., eds. Forest Health Monitoring: national status, trends, and analysis 2015. Gen. Tech. Rep. SRS-213. Asheville, NC: U.S. Department of Agriculture Forest Service, Southern Research Station: 41–60.

Potter, K.M. 2017. Large-scale patterns of forest fire occurrence in the conterminous United States, Alaska, and Hawaii, 2015. In: Potter, K.M.; Conkling, B.L., eds. Forest Health Monitoring: national status, trends, and analysis 2016. Gen. Tech. Rep. SRS-222. Asheville, NC: U.S. Department of Agriculture Forest Service, Southern Research Station: 43–62.

Potter, K.M. 2018. Large-scale patterns of forest fire occurrence in the conterminous United States, Alaska, and Hawaii, 2016. In: Potter, K.M.; Conkling, B.L., eds. Forest Health Monitoring: national status, trends, and analysis 2017. Gen. Tech. Rep. SRS-233. Asheville, NC: U.S. Department of Agriculture Forest Service, Southern Research Station: 45–64.

Potter, K.M. 2019. Large-scale patterns of forest fire occurrence across the 50 United States and the Caribbean territories, 2017. In: Potter, K.M.; Conkling, B.L., eds. Forest Health Monitoring: national status, trends, and analysis 2018. Gen. Tech. Rep. SRS-239. Asheville, NC: U.S. Department of Agriculture Forest Service, Southern Research Station: 51–76.

Potter, K.M. 2020a. Large-scale patterns of forest fire occurrence across the 50 United States and the Caribbean territories, 2018. In: Potter, K.M.; Conkling, B.L., eds. Forest Health Monitoring: national status, trends, and analysis 2019. Gen. Tech. Rep. SRS-250. Asheville, NC: U.S. Department of Agriculture Forest Service, Southern Research Station: 57–82.

Potter, K.M. 2020b. Introduction. In: Potter, K.M.; Conkling, B.L., eds. Forest Health Monitoring: national status, trends, and analysis 2019. Gen. Tech. Rep. SRS-250. Asheville, NC: U.S. Department of Agriculture Forest Service, Southern Research Station: 5–24.

Potter, K.M.; Koch, F.H.; Oswalt, C.M.; Iannone, B.V. 2016. Data, data everywhere: detecting spatial patterns in fine-scale ecological information collected across a continent. Landscape Ecology. 31: 67–84. https://doi.org/10.1007/s10980-015-0295-0.

Pyne, S.J. 2010. America's fires: a historical context for policy and practice. Durham, NC: Forest History Society. 91 p.

Reams, G.A.; Smith, W.D.; Hansen, M.H. [and others]. 2005. The Forest Inventory and Analysis sampling frame. In: Bechtold, W.A.; Patterson, P.L., eds. The enhanced Forest Inventory and Analysis program—national sampling design and estimation procedures. Gen. Tech. Rep. SRS-80. Asheville, NC: U.S. Department of Agriculture Forest Service, Southern Research Station: 11–26.

Richardson, L.A.; Champ, P.A.; Loomis, J.B. 2012. The hidden cost of wildfires: economic valuation of health effects of wildfire smoke exposure in southern California. Journal of Forest Economics. 18(1): 14–35. https://doi.org/10.1016/j.jfe.2011.05.002.

Schmidt, K.M.; Menakis, J.P.; Hardy, C.C. [and others]. 2002. Development of coarse-scale spatial data for wildland fire and fuel management. Gen. Tech. Rep. RMRS-87. Fort Collins, CO: U.S. Department of Agriculture Forest Service, Rocky Mountain Research Station. 41 p. https://doi.org/10.2737/RMRS-GTR-87.

Shima, T.; Sugimoto, S.; Okutomi, M. 2010. Comparison of image alignment on hexagonal and square lattices. In: 2010 IEEE international conference on image processing. [Place of publication unknown]: Institute of Electrical and Electronics Engineers, Inc.: 141–144. https://doi.org/10.1109/ICIP.2010.5654351.

Spencer, P.; Nowacki, G.; Fleming, M. [and others]. 2002. Home is where the habitat is: an ecosystem foundation for wildlife distribution and behavior. Arctic Research of the United States. 16: 6–17.

Tonini, M.; Tuia, D.; Ratle, F. 2009. Detection of clusters using space-time scan statistics. International Journal of Wildland Fire. 18(7): 830–836. https://doi.org/10.1071/WF07167.

Trouet, V.; Taylor, A.H.; Wahl, E.R.; Skinner, C.N. 2010. Fire-climate interactions in the American West since 1400 CE. Geophysical Research Letters. 37(4): L04702. https://doi.org/10.1029/2009GL041695.

U.S. Department of Agriculture (USDA) Forest Service. 2008. National forest type data development. http://svinetfc4.fs.fed.us/rastergateway/forest_type/. [Date accessed: May 13, 2008].

U.S. Department of Agriculture (USDA) Forest Service. 2020. Fire detection GIS data. https://fsapps.nwcg.gov/afm/gisdata.php. [Date accessed: June 24, 2020].

White, D.; Kimerling, A.J.; Overton, W.S. 1992. Cartographic and geometric components of a global sampling design for environmental monitoring. Cartography and Geographic Information Systems. 19(1): 5–22. https://doi.org/10.1559/152304092783786636.